

Supporting information

Highly Selective, Potent and Oral mTOR Inhibitor for Treatment of Cancer as Autophagy Inducer

Qingxiang Guo,^{±1} Chenhua Yu,^{±1} Chao Zhang,¹ Yongtao Li,¹ Tianqi Wang,¹ Zhi Huang,¹ Xin Wang,¹ Wei Zhou,¹ Yao Li,¹ Zhongxiang Qin,¹ Cheng Wang,¹ Ruifang Gao,¹ Yongwei Nie,¹ Yakun Ma,¹ Yi Shi,¹ Jianyu Zheng,⁴ Shengyong Yang,⁵ Yan Fan*^{1,2} and Rong Xiang*^{1,3}

¹ School of Medicine, Nankai University, 94 Weijin Road, Tianjin 300071, China

² International Collaborative Laboratory of Biomedicine of the Ministry of Education, 94 Weijin Road, Tianjin 300071, China

³ 2011 Project Collaborative Innovation Center for Biotherapy of Ministry of Education, 94 Weijin Road, Tianjin 300071, China

⁴ State Key Laboratory and Institute of Elemento-Organic Chemistry, Collaborative Innovation Center of Chemical Science and Engineering, Nankai University, Tianjin 300071, China.

⁵ State Key Laboratory of Biotherapy and Cancer Center, West China Hospital, Sichuan University and Collaborative Innovation Center for Biotherapy, Chengdu 610041, China

* **Corresponding authors:** Yan Fan*: Tel: +86 22 23509482. E-mail: yanfan@nankai.edu.cn; Rong Xiang*: Tel: +86 22 23509482. E-mail: rxiang@nankai.edu.cn.

Author Contributions:[†]Qingxiang Guo and Chenhua Yu contributed equally to this work.

Table of Contents:

Figure S1 Literature reported dual PI3K/mTOR and selective ATP-competitive mTOR inhibitors.....	S3
Table S1 Cell inhibitory activity of 9a in different cell lines.....	S4
Table S2 T-47D inhibitory activities of compounds 9a-b , 9m-n , 9i-l , 9v-x , 9z-cc , at 5 μ M and 1 μ M.....	S5
Table S3 IC ₅₀ values of 9a , 9m , 9i , 9j , 9v , 9z inhibit T-47D and MCF7 cell lines.....	S6
Table S4 Kinase Profiling Results of compound 9m	S7
Figure S2 Representation of the predicted binding modes of inactive compound 9af with mTOR kinase domain.....	S13
Table S5 Docking scores of some synthesized compounds.....	S14
Protein plasma binding and stability	S15
Table S6. Plasma protein binding of 9m in rabbit and human plasma.....	S15
Copy of ¹H- and ¹³C-NMR Spectra for 9m	S16
Copy of MS Spectra for 9m	S17
HPLC Purity Analysis for Compound 9m	S18
References	S18

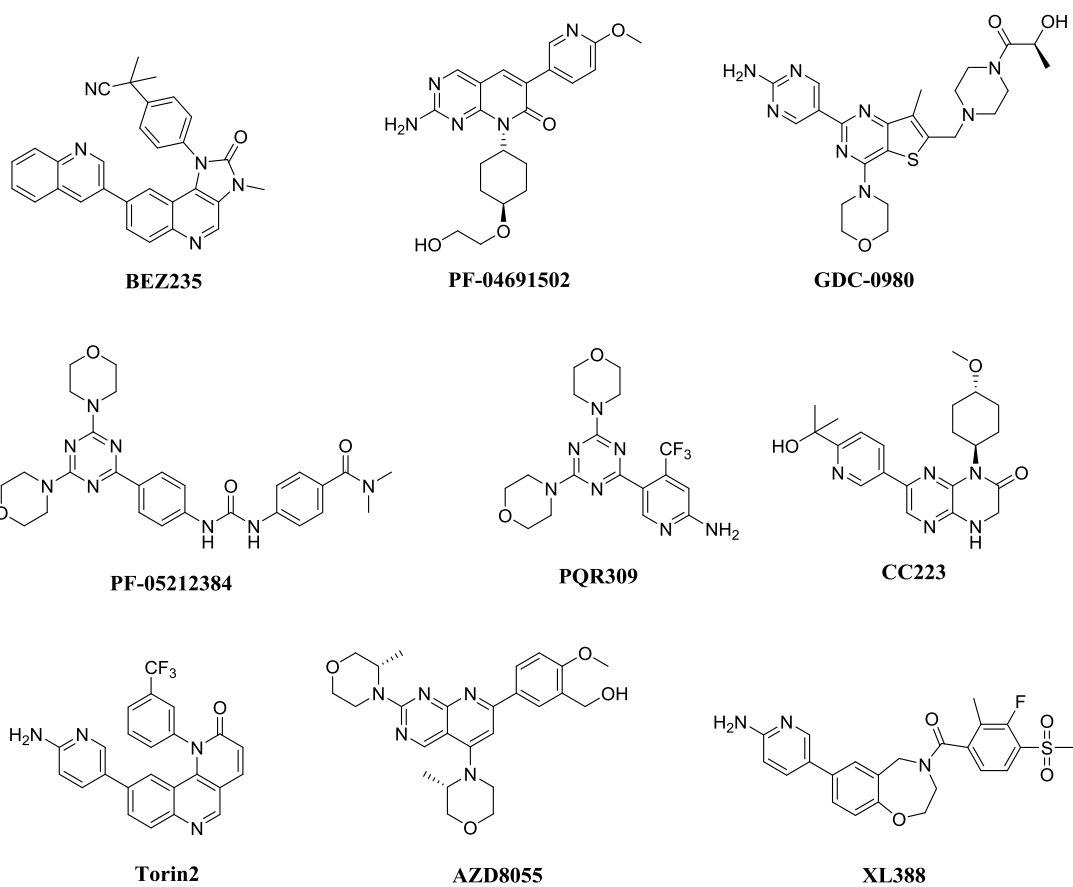


Figure S1 Literature reported dual PI3K/mTOR and selective ATP-competitive mTOR inhibitors.

Table S1. Cell inhibitory activity of 9a in different cell lines

Compound	Cell lines	IC ₅₀ (nM)
9a	MCF7	556
	T-47D	578
	MDA-MB-231	5995
	Hela	1034
	Siha	1311
	Skov3	2485
	OVCAR-5	1218
	H460	596

Table S2 T-47D inhibitory activities of compounds **9a-b**, **9m-n**, **9i-l**, **9v-x**, **9z-ac**, **9ag**,

12a-d at 5 μ M and 1 μ M

Compound	5 μ M inhibiton ratio(%)	1 μ M inhibiton ratio(%)
9a	90	51
9b	83	41
9m	100	82
9n	71	60
9i	80	15
9j	61	0.5
9k	53	0.3
9l	79	41
9v	85	54
9w	85	15
9x	90	39
9z	95	69
9aa	90	55
9ab	48	13
9ac	78	22
9ag	59	27
12a	59	35
12b	43	18
12c	43	24
12d	67	61

Table S3 IC₅₀^a values of **9a-b**, **9m**, **9i**, **9j**, **9x**, **9z**, **9aa**, **9ac**, **12d** inhibit T-47D and MCF7 cell lines

compound	IC ₅₀ (T-47D)	IC ₅₀ (MCF7)
9a	991	1845
9b	1296	277
9m	205	103
9i	517	538
9j	1785	5573
9x	1658	3801
9z	1785	5573
9aa	910	5365
9ac	5738	2162
12d	1094	542

^a IC₅₀: the dose that inhibits 50% of the cells present in the control wells. The IC₅₀ values are the average of at least three independent determinations.

Table S4 Kinase Profiling Results of compound **9m^a**

kinase	Inhibition % @ 1 μ M	kinase	Inhibition % @ 1 μ M
Abl(h)	22	MEKK3(h)	6
Abl(m)	17	MELK(h)	48
Abl (H396P) (h)	17	Mer(h)	5
Abl (M351T)(h)	11	Met(h)	-6
Abl (Q252H) (h)	17	Met(D1246H)(h)	14
Abl(T315I)(h)	-16	Met(D1246N)(h)	0
Abl(Y253F)(h)	9	Met(M1268T)(h)	-5
ACK1(h)	9	Met(Y1248C)(h)	7
ACTR2(h)	5	Met(Y1248D)(h)	4
ALK(h)	4	Met(Y1248H)(h)	1
ALK1(h)	4	MINK(h)	7
ALK2(h)	7	MKK4(m)	6
ALK4(h)	1	MKK6(h)	1
ALK6(h)	1	MKK7 β (h)	-11
Arg(h)	2	MLCK(h)	-4
AMPK α 1(h)	1	MLK1(h)	5
AMPK α 2(h)	0	MLK2(h)	1
A-Raf(h)	1	Mnk2(h)	9
Arg(m)	7	MOK(h)	7
ARK5(h)	-5	MRCK α (h)	-1
ASK1(h)	8	MRCK β (h)	-7
Aurora-A(h)	0	MSK1(h)	2
Aurora-B(h)	4	MSK2(h)	-7
Aurora-C(h)	-2	MSSK1(h)	6
Axl(h)	3	MST1(h)	-3
Blk(h)	30	MST2(h)	0
Blk(m)	28	MST3(h)	-11
BMPR2(h)	-11	MST4(h)	-8
Bmx(h)	2	MuSK(h)	5
BRK(h)	0	MYLK2(h)	10
BrSK1(h)	9	MYO3B(h)	-3
BrSK2(h)	-2	NDR2(h)	-11
BTK(h)	-4	NEK1(h)	-8
BTK(R28H)(h)	0	NEK2(h)	-1
B-Raf(h)	5	NEK4(h)	9
B-Raf(V599E)(h)	17	NEK3(h)	-1
CaMKI(h)	10	NEK6(h)	-10
CaMKI β (h)	-12	NEK7(h)	-12
CaMKI γ (h)	-4	NEK9(h)	-8

CaMKII α (h)	2	NIM1(h)	-9
CaMKII β (h)	8	NEK11(h)	0
CaMKII γ (h)	-8	NLK(h)	6
CaMKI δ (h)	-7	NUAK2(h)	-4
CaMKII δ (h)	2	p70S6K(h)	-8
CaMKIV(h)	-12	PAK1(h)	-1
CaMKK1(h)	-2	PAK2(h)	-6
CaMKK2(h)	-3	PAK4(h)	-1
Cdc7/cyclinB1(h)	3	PAK3(h)	-5
CDK1/cyclinB(h)	5	PAK5(h)	1
CDK2/cyclinA(h)	2	PAK6(h)	3
CDK2/cyclinE(h)	0	PAR-1B α (h)	4
CDK3/cyclinE(h)	2	PASK(h)	7
CDK4/cyclinD3(h)	-6	PEK(h)	-9
CDK5/p25(h)	-3	PDGFR α (h)	-2
CDK5/p35(h)	4	PDGFR α (D842V)(h)	1
CDK6/cyclinD3(h)	2	PDGFR α (V561D)(h)	-14
CDK7/cyclinH/MAT1(h)	5	PDGFR β (h)	-3
CDK9/cyclin T1(h)	0	PDHK4(h)	-1
CDK12/cyclinK(h)	6	PDK1(h)	-5
CDK13/cyclinK(h)	-12	PhK γ 1(h)	8
CDK14/cyclinY(h)	-6	PhK γ 2(h)	-2
CDK18/cyclinY(h)	1	Pim-1(h)	14
CDKL1(h)	11	Pim-2(h)	-9
CDKL2(h)	2	Pim-3(h)	8
CDKL3(h)	12	PKA(h)	-11
CDKL4(h)	12	PKA α β (h)	9
ChaK1(h)	1	PKB α (h)	-4
CHK1(h)	1	PKB β (h)	4
CHK2(h)	-1	PKB γ (h)	-10
CHK2(I157T)(h)	0	PKC α (h)	4
CHK2(R145W)(h)	-7	PKC β I(h)	6
CK1 γ 1(h)	5	PKC β II(h)	13
CK1 γ 2(h)	6	PKC γ (h)	-1
CK1 γ 3(h)	-12	PKC δ (h)	2
CK1 δ (h)	13	PKC ϵ (h)	2
CK1(y)	15	PKC η (h)	1
CK2(h)	-1	PKC ι (h)	4
CK2 α 1(h)	5	PKC μ (h)	-6
CK2 α 2(h)	-7	PKC θ (h)	11
CLIK1(h)	6	PKC ζ (h)	-8
CLK1(h)	28	PKD2(h)	6
CLK2(h)	18	PKD3(h)	-6

CLK3(h)	-1	PKG1 α (h)	7
CLK4(h)	30	PKG1 β (h)	-4
cKit(h)	-4	PKR(h)	1
cKit(D816V)(h)	2	Plk1(h)	-2
cKit(D816H)(h)	0	Plk3(h)	5
cKit(V560G)(h)	10	Plk4(h)	-3
cKit(V654A)(h)	1	PRAK(h)	2
CSK(h)	-3	PRKG2(h)	-5
c-RAF(h)	-3	PRK1(h)	-6
cSRC(h)	14	PRK2(h)	0
DAPK1(h)	14	PrKX(h)	3
DAPK2(h)	-8	PRP4(h)	-8
DCAMKL2(h)	6	PTK5(h)	6
DCAMKL3(h)	3	Pyk2(h)	0
DDR1(h)	-9	Ret(h)	7
DDR2(h)	-5	Ret (V804L)(h)	4
DMPK(h)	-8	Ret(V804M)(h)	11
DRAK1(h)	1	RIPK1(h)	-5
DRAK2(h)	-11	RIPK2(h)	8
DYRK1A(h)	5	ROCK-I(h)	1
DYRK1B(h)	7	ROCK-II(h)	-15
DYRK2(h)	-15	ROCK-II(r)	10
DYRK3(h)	4	Ron(h)	0
eEF-2K(h)	3	Ros(h)	-5
EGFR(h)	3	Rse(h)	-10
EGFR(L858R)(h)	37	Rsk1(h)	-14
EGFR(L861Q)(h)	32	Rsk1(r)	5
EGFR(T790M)(h)	-4	Rsk2(h)	-2
EGFR(T790M,L858R)(h)	32	Rsk3(h)	-14
EphA1(h)	2	Rsk4(h)	-5
EphA2(h)	-4	SAPK2a(h)	-10
EphA3(h)	-3	SAPK2a(T106M)(h)	-1
EphA4(h)	4	SAPK2b(h)	-3
EphA5(h)	-9	SAPK3(h)	-14
EphA7(h)	-1	SAPK4(h)	-1
EphA8(h)	-8	SBK1(h)	5
EphB2(h)	-10	SGK(h)	0
EphB1(h)	-22	SGK2(h)	-6
EphB3(h)	7	SGK3(h)	1
EphB4(h)	0	SIK(h)	-7
ErbB2(h)	18	SIK2(h)	-2
ErbB4(h)	8	SIK3(h)	-5
FAK(h)	-1	SLK(h)	-2

Fer(h)	4	Snk(h)	1
Fes(h)	1	SNRK(h)	-5
FGFR1(h)	-4	Src(1-530)(h)	6
FGFR1(V561M)(h)	4	Src(T341M)(h)	-2
FGFR2(h)	-1	SRPK1(h)	-4
FGFR2(N549H)(h)	6	SRPK2(h)	1
FGFR3(h)	-5	STK16(h)	2
FGFR4(h)	-3	STK25(h)	-1
Fgr(h)	4	STK32A(h)	4
Flt1(h)	29	STK32B(h)	4
Flt3(D835Y)(h)	16	STK32C(h)	0
Flt3(h)	29	STK33(h)	5
Flt4(h)	22	Syk(h)	-11
Fms(h)	0	TAF1L(h)	0
Fms(Y969C)(h)	17	TAK1(h)	-16
Fyn(h)	4	TAO1(h)	-3
GCK(h)	10	TAO2(h)	0
GCN2(h)	-17	TAO3(h)	4
GRK1(h)	2	TBK1(h)	0
GRK2(h)	4	Tec(h) activated	4
GRK3(h)	-3	TGFBR1(h)	-5
GRK5(h)	0	TGFBR2(h)	3
GRK6(h)	1	Tie2 (h)	-1
GRK7(h)	-9	Tie2(R849W)(h)	4
GSK3 α (h)	-1	Tie2(Y897S)(h)	1
GSK3 β (h)	2	TLK1(h)	-11
Haspin(h)	4	TLK2(h)	-4
Hck(h)	3	TNIK(h)	-12
Hck(h) activated	-4	TRB2(h)	6
HIPK1(h)	-4	TrkA(h)	40
HIPK2(h)	-4	TrkB(h)	-26
HIPK3(h)	4	TrkC(h)	-23
HIPK4(h)	11	TSSK1(h)	-1
HPK1(h)	3	TSSK2(h)	-9
HRI(h)	-10	TSSK3(h)	-4
ICK(h)	-2	TSSK4(h)	5
IGF-1R(h)	-21	TTBK1(h)	-12
IGF-1R(h), activated	-3	TTBK2(h)	-3
IKK α (h)	-3	TTK(h)	3
IKK β (h)	2	Txk(h)	12
IKK ϵ (h)	-3	TYK2(h)	22
IR(h)	-10	ULK1(h)	4
IR(h), activated	7	ULK2(h)	-4

IRE1(h)	3	ULK3(h)	-2
IRR(h)	2	VRK1(h)	-2
IRAK1(h)	4	VRK2(h)	7
IRAK4(h)	9	Wee1(h)	-9
Itk(h)	38	Wee1B(h)	-10
JAK1(h)	34	WNK1(h)	-2
JAK2(h)	29	WNK2(h)	-3
JAK3(h)	0	WNK3(h)	-5
JNK1 α 1(h)	7	Yes(h)	10
JNK2 α 2(h)	0	ZAP-70(h)	-18
JNK3(h)	9	ZIPK(h)	-7
KDR(h)	5	PIP4K2 α (h)	0
Lck(h)	33	PIP5K1 α (h)	29
Lck(h) activated	2	PIP5K1 γ (h)	4
LIMK1(h)	-3	ATM(h)	96
LIMK2(h)	9	ATR/ATRIP(h)	24
LKB1(h)	-4	DNA-PK(h)	95
LOK(h)	5	PI3 Kinase (p110 β /p85 α)(h)	7
Lyn(h)	0	PI3 Kinase (p120 γ)(h)	4
Lyn(m)	-1	PI3 Kinase (p110 δ /p85 α)(h)	9
LRRK2(h)	0	PI3 Kinase (p110 α /p85 α)(m)	17
LTK(h)	5	PI3 Kinase (p110 α /p65 α)(m)	9
MAK(h)	-5	PI3 Kinase (p110 α (E545K)/p85 α)(m)	9
MAPK1(h)	-2	PI3 Kinase (p110 α (H1047R)/p85 α)(m)	7
MAPK2(h)	-8	PI3 Kinase (p110 β /p85 β)(m)	8
MAPK2(m)	3	PI3 Kinase (p110 β /p85 α)(m)	5
MAP4K3(h)	5	PI3 Kinase (p110 δ /p85 α)(m)	4
MAP4K4(h)	6	PI3 Kinase (p110 α (E542K)/p85 α)(m)	10
MAP4K5(h)	-11	PI3 Kinase (p110 α /p85 α)(h)	10
MAPKAP-K2(h)	-4	PI3 Kinase (p110 α (E542K)/p85 α)(h)	11
MAPKAP-K3(h)	1	PI3 Kinase (p110 α (H1047R)/p85 α)(h)	2
MEK1(h)	-3	PI3 Kinase (p110 α (E545K)/p85 α)(h)	13
MEK2(h)	0	PI3 Kinase (p110 α /p65 α)(h)	5
MARK1(h)	1	PI3KC2 α (h)	4
MARK3(h)	-7	mTOR(h)	100
MARK4(h)	-2	mTOR/FKBP12(h)	100
MEKK2(h)	-6		

^avalues were determined using KinaseProfiler by Eurofins. The data represent the mean values of two independent experiments

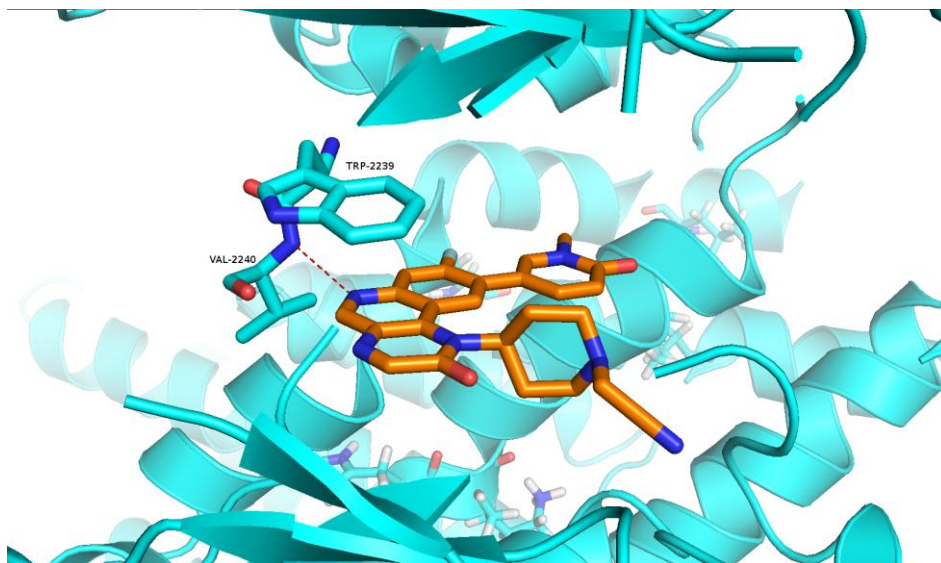


Figure S2. Representation of the predicted binding modes of inactive compound **9af** with mTOR kinase domain (PDB code: 4jsx). Proposed binding modes of compound **9af** with mTOR. **9af** is shown in orange, mTOR backbone is shown in cyan. Hydrogen bond is shown in red.

Table S5 Docking scores of some synthesized compounds

Compound	Gold. goldscore. fitness
9a	74.8032
6h	68.5161
8a	63.0639
8f	72.2551
9c	65.5765
9e	69.1865
9g	71.5147
9k	78.1104
9m	80.4574
9p	74.6269
9s	70.2468
9y	62.3651
9ab	75.5808
9af	55.4318
9ag	78.5477
12d	76.2973

Table S6. Plasma protein binding of **9m** in rabbit and human plasma

%Bound								%Compound remaining at 4h	
Rabbit				Human				Rabbit	Human
R1	R2	R3	Mean ±SD	R1	R2	R3	Mean ±SD	91	92
63.8	55.9	60.5	60.1 ±3.9	63.4	66.1	62.6	64.0 ±1.8		

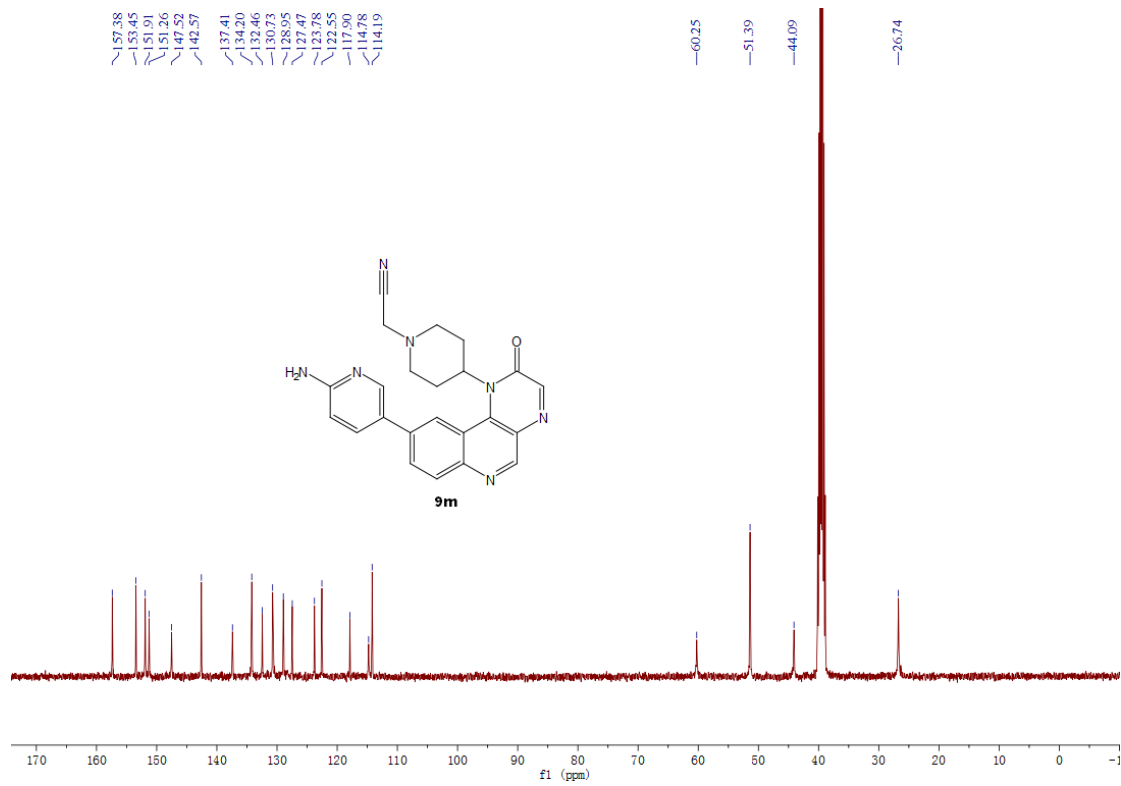
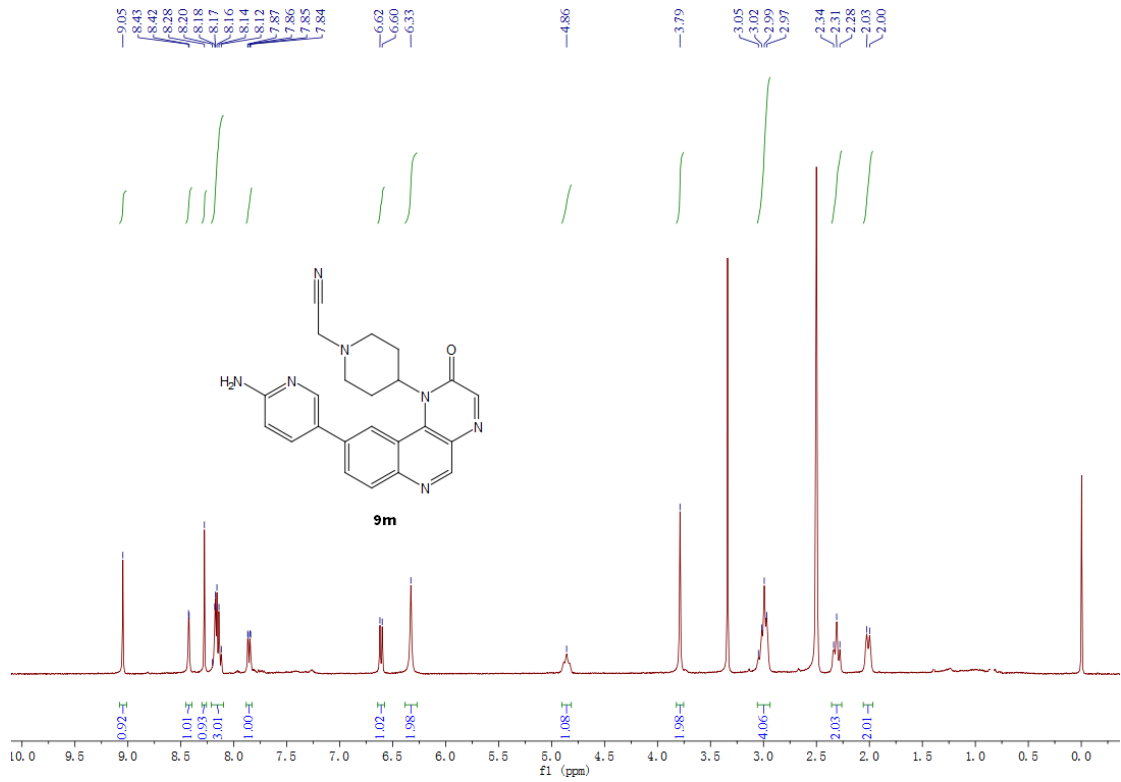
Protein plasma binding and stability.^{1,2} The serum protein binding rate of **9m** was determined in fresh rabbit and human sera by the equilibrium dialysis method. Fresh rabbit and human serum (1 mL) was separately sealed into the dialysis bag (MWCO: 8000-14000 Da) and the bag was immersed into 20 mL **9m** phosphate-buffered saline (PBS, pH = 7.4) solution at the concentration of 4 μM (N = 3). Then the dialysis was performed at 37 °C with shaking at 200 RPM for 4 h. After 4 h, 100 μL of serum samples in the dialysis bag and samples in the dialysis solution(out of the dialysis bag) was separately collected for LC-MS/MS analysis. Protein binding rate was calculated using the following equation.

$$\% \text{ bound} = \frac{\text{concentration of } \mathbf{9m} \text{ in serum} - \text{concentration of } \mathbf{9m} \text{ in dialysis solution}}{\text{concentration of } \mathbf{9m} \text{ in serum}} \times 100$$

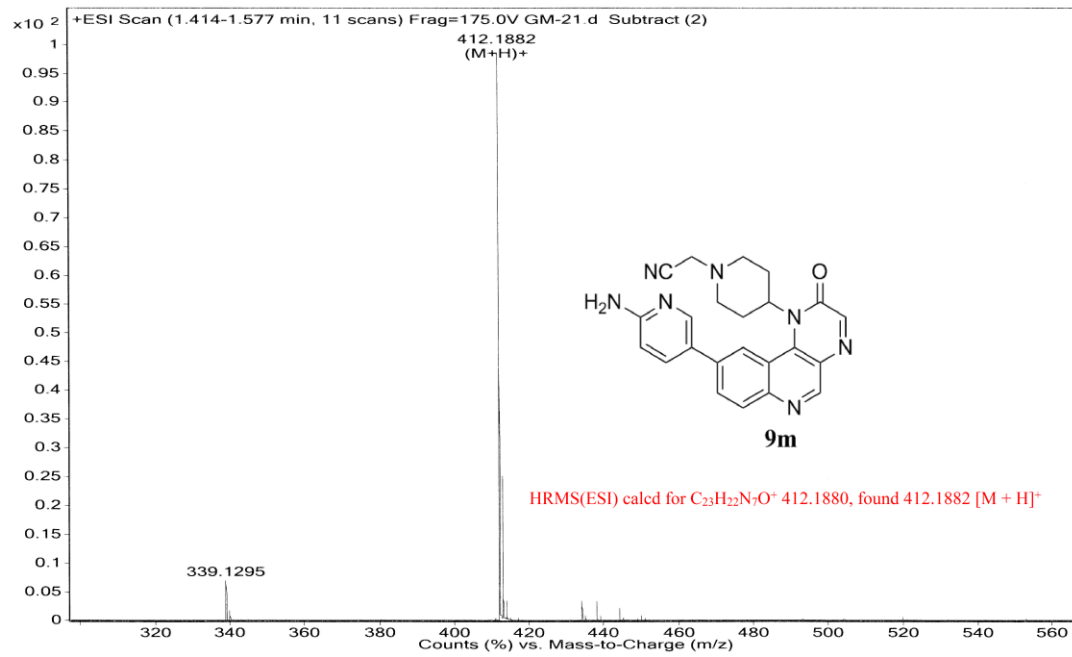
The stability of **9m** in serum: **9m** was added to six tubes. Three aliquots were frozen immediately (0-hour sample). The other three aliquots were treated as the above dialysis method at 37 °C with shaking at 200 RPM for 4 h. Following dialysis, 100 μL of serum samples in the dialysis bag was collected (4-hour sample). Samples were analyzed by LC/MS/MS. Serum stability was assessed using following equation.

$$\% \text{ stability} = \frac{\text{peak area of 4-hour sample}}{\text{peak area of 0-hour sample}} \times 100$$

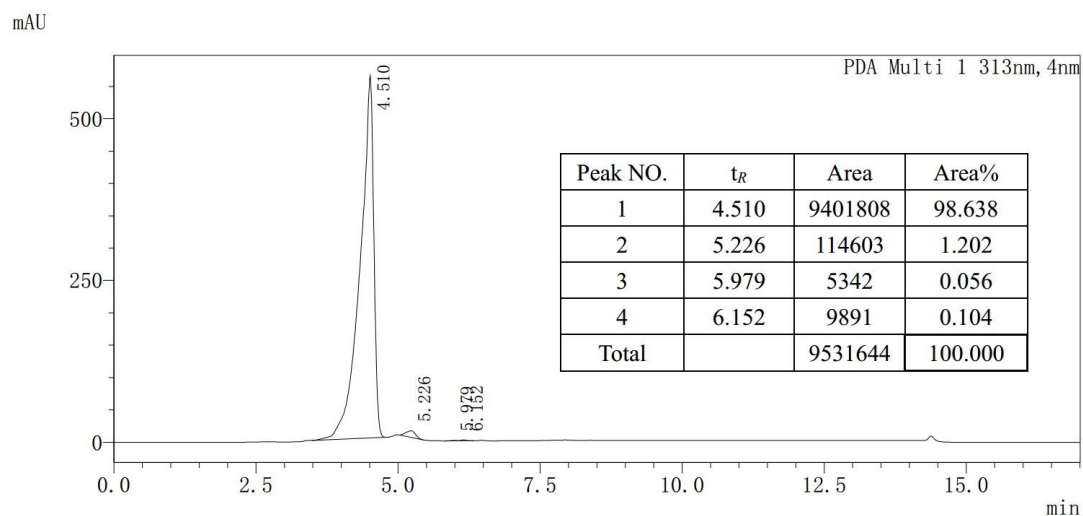
Copy of ¹H- and ¹³C-NMR Spectra for 9m



Copy of MS Spectra for 9m



HPLC Purity Analysis for Compound 9m



Reference:

1. Wang, H.-Y.; Qin, Y.; Li, H.; Roman, L. J.; Mart ásek, P.; Poulos, T. L.; Silverman, R. B. Potent and selective human neuronal nitric oxide synthase inhibition by optimization of the 2-aminopyridine-based scaffold with a pyridine linker. *J. Med. Chem.* **2016**, *59*, 4913-4925.
2. Ellsworth, B. A.; Sher, P. M.; Wu, X.; Wu, G.; Sulsky, R. B.; Gu, Z.; Murugesan, N.; Zhu, Y.; Yu, G.; Sitkoff, D. F.; Carlson, K. E.; Kang, L.; Yang, Y.; Lee, N.; Baska, R. A.; Keim, W. J.; Cullen, M. J.; Azzara, A. V.; Zuvich, E.; Thomas, M. A.; Rohrbach, K. W.; Devenny, J. J.; Godonis, H. E.; Harvey, S. J.; Murphy, B. J.; Everlof, G. G.; Stetsko, P. I.; Gudmundsson, O.; Johnghar, S.; Ranasinghe, A.; Behnia, K.; Pelleymounter, M. A.; Ewing, W. R. Reductions in log p improved protein binding and clearance predictions enabling the prospective design of cannabinoid receptor (cb1) antagonists with desired pharmacokinetic properties. *J. Med. Chem.* **2013**, *56*, 9586-9600.